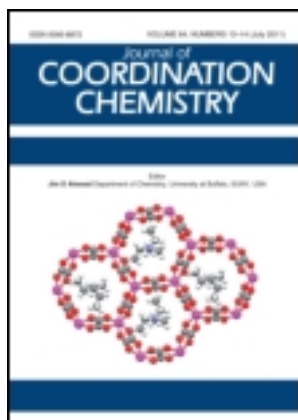


This article was downloaded by: [Renmin University of China]

On: 13 October 2013, At: 10:41

Publisher: Taylor & Francis

Informa Ltd Registered in England and Wales Registered Number: 1072954 Registered office: Mortimer House, 37-41 Mortimer Street, London W1T 3JH, UK



Journal of Coordination Chemistry

Publication details, including instructions for authors and subscription information:

<http://www.tandfonline.com/loi/gcoo20>

Two new 2-D coordination polymers based on a purine-containing carboxylate

Xin-Qi Liu^{a, b}, Zhong-Yuan Li^c, Xiao-Ju Yuan^a & Ben-Lai Wu^a

^a Department of Chemistry, Zhengzhou University, Zhengzhou 450001, P.R. China

^b Henan Vocational College of Chemical Technology, Zhengzhou 450052, P.R. China

^c Shenzhen Academy of Metrology & Quality Inspection, Shenzhen 518055, P.R. China

Accepted author version posted online: 23 Aug 2012. Published online: 10 Sep 2012.

To cite this article: Xin-Qi Liu, Zhong-Yuan Li, Xiao-Ju Yuan & Ben-Lai Wu (2012) Two new 2-D coordination polymers based on a purine-containing carboxylate, *Journal of Coordination Chemistry*, 65:21, 3721-3730, DOI: [10.1080/00958972.2012.724172](https://doi.org/10.1080/00958972.2012.724172)

To link to this article: <http://dx.doi.org/10.1080/00958972.2012.724172>

PLEASE SCROLL DOWN FOR ARTICLE

Taylor & Francis makes every effort to ensure the accuracy of all the information (the "Content") contained in the publications on our platform. However, Taylor & Francis, our agents, and our licensors make no representations or warranties whatsoever as to the accuracy, completeness, or suitability for any purpose of the Content. Any opinions and views expressed in this publication are the opinions and views of the authors, and are not the views of or endorsed by Taylor & Francis. The accuracy of the Content should not be relied upon and should be independently verified with primary sources of information. Taylor and Francis shall not be liable for any losses, actions, claims, proceedings, demands, costs, expenses, damages, and other liabilities whatsoever or howsoever caused arising directly or indirectly in connection with, in relation to or arising out of the use of the Content.

This article may be used for research, teaching, and private study purposes. Any substantial or systematic reproduction, redistribution, reselling, loan, sub-licensing, systematic supply, or distribution in any form to anyone is expressly forbidden. Terms &

Conditions of access and use can be found at <http://www.tandfonline.com/page/terms-and-conditions>

Two new 2-D coordination polymers based on a purine-containing carboxylate

XIN-QI LIU^{†,‡}, ZHONG-YUAN LI[§], XIAO-JU YUAN[†] and BEN-LAI WU^{*†}

[†]Department of Chemistry, Zhengzhou University, Zhengzhou 450001, P.R. China

[‡]Henan Vocational College of Chemical Technology, Zhengzhou 450052, P.R. China

[§]Shenzhen Academy of Metrology & Quality Inspection, Shenzhen 518055, P.R. China

(Received 1 January 2012; in final form 20 June 2012)

A purine-containing multifunctional ligand, 2-(6-oxo-6H-purin-1(9H)-yl)acetic acid (**HL**), and two new 2-D coordination polymers, $[\text{Co}(\text{L})_2(\text{H}_2\text{O})_2]_n \cdot 2n\text{H}_2\text{O}$ (**1**) and $[\text{Ni}(\text{L})_2(\text{H}_2\text{O})_2]_n \cdot 2n\text{H}_2\text{O}$ (**2**), were synthesized and characterized. Polymers **1** and **2** have isomorphous structures with (4,4)-connected topologies composed of left- and right-handed metal–organic helices sharing common metal centers. Two helical conformations in the same net are stabilized by strong π – π stacking interactions between purine groups. Through direct and water-mediated interlayer hydrogen-bond interactions those layers are assembled into stable 3-D supermolecules where slight differences in the strength of hydrogen bonds and coordination bonds result in their decomposition behaviors.

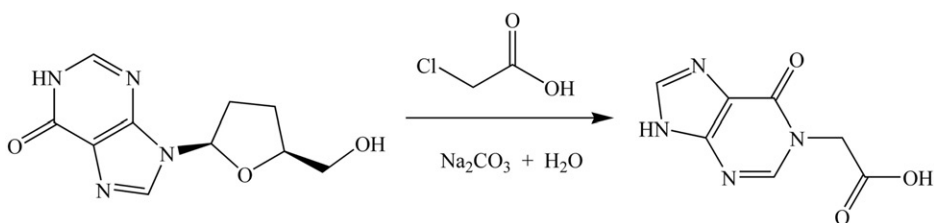
Keywords: Purine-containing ligand; Coordination polymers; Metal–organic helices; Thermal stability

1. Introduction

Bioactive N-heterocyclic compounds, such as purine and its derivatives, are probes to investigate biological systems for therapeutics and spacers in supramolecular self-assembly to construct models for understanding many natural and synthetic systems [1–7]. For example, purine derivatives can selectively recognize the sequence, configuration, and region of nucleic acid, which has a big influence on the design of new metal drugs and plays an important role in biology and medicine [4, 5]. They are endowed with multiple binding sites for assembly of higher dimensional supermolecules through coordination, hydrogen-bonding, and π – π interactions [8–10], providing a good chance for construction of purine-containing supermolecules which can be used to investigate the influence of metal ions on the structures and functions of resulting assemblies.

Carboxylic acids, especially aromatic acids, have attracted interest in construction of metal–organic frameworks (MOFs), owing to diverse coordination modes and hydrogen bonds originating from carboxyl groups [11]. It is a facile way to functionalize heterocyclic compounds through attaching an acetic group into the aromatic backbone.

*Corresponding author. Email: wbl@zzu.edu.cn

Scheme 1. Schematic representation of the synthesis of **HL**.

The modification adds interesting features into the ligands [12]. That is, the flexible acetic acid group fused with rigid heterocyclic skeleton increases the coordination and hydrogen-bonding sites and improves flexibility, which is very important in crystal engineering to obtain high-dimensional MOFs. Distortion of carboxyl from the conjugated heterocycle makes forming helical coordination polymers easier.

We designed and synthesized a new purine-containing carboxylic acid, 2-(6-oxo-6H-purin-1(9H)-yl)acetic acid (**HL**), shown in scheme 1. By using the multifunctional ligand to assemble with Co^{II} and Ni^{II} , respectively, two new 2-D coordination polymers, $[\text{Co}(\text{L})_2(\text{H}_2\text{O})_2]_n \cdot 2n\text{H}_2\text{O}$ (**1**) and $[\text{Ni}(\text{L})_2(\text{H}_2\text{O})_2]_n \cdot 2n\text{H}_2\text{O}$ (**2**), were obtained. Purine-containing MOFs have been little reported [8–10, 13].

2. Experimental

2.1. General information and materials

All chemicals purchased were of reagent grade or better and used without purification. IR spectra (KBr pellets) were recorded on a Nicolet NEXUS 470 FT-IR spectrophotometer from 400 to 4000 cm^{-1} . Elemental analyses for C, H, and N were performed with a Carlo-Erba 1106 elemental analyzer. ^1H NMR spectrum was recorded on a Bruker DPX-300 spectrometer at 300 MHz. Thermal analysis curves were scanned from 30°C to 650°C under air on a STA 409 PC thermal analyzer. Electronic absorption spectra were recorded on a Unico-2102 UV-Vis spectrometer. X-ray powder diffraction (XPRD) patterns of the samples were recorded by a RIGAKU-DMAX2500 X-ray diffractometer with $\text{Cu-K}\alpha$ radiation.

2.2. Syntheses

2.2.1. Synthesis of 2-(6-oxo-6H-purin-1(9H)-yl)acetic acid (HL). Sodium carbonate (2.12 g, 20.0 mmol) was slowly added to an aqueous solution (20 mL) of chloroacetic acid (1.14 g, 12.0 mmol) under stirring and heating, and then dideoxyinosine (2.36 g, 10.0 mmol) was added to the mixture. After refluxing for 5 h, the resultant mixture was acidified to pH of 2–3 by dropwise addition of hydrochloric acid. Following filtration, the resulting precipitate was washed with methanol and dried under an infrared lamp. White powder was obtained (yield 65%). IR (KBr, $\nu\text{ cm}^{-1}$): 3129(m), 3064(m), 1730(vs), 1685(vs), 1590(m), 1557(m), 1391(m), 1230(s), 1195(s), 954(m),

Table 1. Crystal data and structure refinement for **1** and **2**.

	1	2
Empirical formula	C ₁₄ H ₁₈ N ₈ O ₁₀ Co	C ₁₄ H ₁₈ N ₈ O ₁₀ Ni
Formula weight	517.29	517.07
Crystal system	Monoclinic	Monoclinic
Space group	<i>P</i> 2 ₁ / <i>c</i>	<i>P</i> 2 ₁ / <i>c</i>
Unit cell dimensions (Å, °)		
<i>a</i>	7.5417(15)	7.4845(15)
<i>b</i>	9.0526(18)	8.7900(18)
<i>c</i>	13.336(3)	13.355(3)
α	90	90
β	95.06(3)	95.24(3)
γ	90	90
Volume (Å ³), <i>Z</i>	906.9(3), 2	874.9(3), 2
Calculated density (g cm ⁻³)	1.894	1.963
Goodness-of-fit on <i>F</i> ²	1.195	1.078
Final <i>R</i> indices	<i>R</i> ₁ = 0.0666	<i>R</i> ₁ = 0.0509
[<i>I</i> > 2σ(<i>I</i>)]	<i>wR</i> ₂ = 0.1685	<i>wR</i> ₂ = 0.1393
Largest difference peak and hole (e Å ⁻³)	0.536 and -0.904	0.431 and -0.532

788(m), 535(m). Anal. Calcd for C₇H₆N₄O₃ (%): C, 43.31; H, 3.11; N, 28.86. Found (%): C, 43.42; H, 3.17; N, 28.45. ¹H NMR (DMSO-*d*₆, 300 MHz) δ (ppm): 3.34 (2H, CH₂), 7.98–8.10 (2H, C_(purin)H), 12.24 (1H, COOH), 13.33. (1H, N_(imidazole)H).

2.2.2. Synthesis of [Co(L)₂(H₂O)₂]_{*n*}·2*n*H₂O (1**).** A mixture of CoSO₄·7H₂O (0.0281 g, 0.1 mmol), **HL** (0.0388 g, 0.2 mmol), methanol (2 mL), and H₂O (6 mL) was stirred for 20 min, and then filtered. After slow evaporation of the resulting solution for 3 weeks without disturbance, pink block crystals were obtained (yield 78%). IR (KBr, ν cm⁻¹): 3147(m), 1663(vs), 1628(s), 1561(s), 1381(s), 1301(m), 1232(m), 1182(m), 952(m), 791(m), 552(m). Anal. Calcd for C₁₄H₁₈N₈O₁₀Co (%): C, 32.51; H, 3.51; N, 21.66. Found (%): C, 32.85; H, 3.47; N, 21.42.

2.2.3. Synthesis of [Ni(L)₂(H₂O)₂]_{*n*}·2*n*H₂O (2**).** According to the same synthesis procedure of **1**, **2** was prepared with replacement of CoSO₄·7H₂O with NiSO₄·6H₂O. IR (KBr, ν cm⁻¹): 3149(m), 1663(vs), 1629(s), 1562(s), 1383(s), 1301(m), 1232(m), 955(m), 836(m), 651(m), 554(m). Anal. Calcd for C₁₄H₁₈N₈O₁₀Ni (%): C, 32.52; H, 3.51; N, 21.66. Found (%): C, 32.23; H, 3.65; N, 21.87.

2.3. Single-crystal structure determination

Crystallographic data of these crystals were collected at 293(2) K on a Siemens SMART CCD diffractometer equipped with a graphite crystal and incident beam monochromator using Mo-Kα radiation (λ = 0.71073 Å). Absorption corrections were applied by using SADABS. The structures were solved with direct methods, and all calculations were performed using the SHELXTL program package [14]. All non-hydrogen atoms were refined anisotropically. Crystal data are summarized in table 1. Selected bond lengths and angles and hydrogen bonds are listed in tables 2 and 3.

Table 2. Selected bond lengths (Å) and angles (°) for **1** and **2**.

1			
Co1–O4A	2.090(4)	Co1–O4	2.090(4)
Co1–O3B	2.103(4)	Co1–O3C	2.103(4)
Co1–N1A	2.201(5)	Co1–N1	2.201(5)
O4A–Co1–O4	180.0	O4A–Co1–O3B	91.57(16)
O4–Co1–O3B	88.43(16)	O4A–Co1–O3C	88.43(16)
O4–Co1–O3C	91.57(16)	O3B–Co1–O3C	180.0
O4A–Co1–N1A	92.72(18)	O4–Co1–N1A	87.28(18)
O3B–Co1–N1A	82.76(17)	O3C–Co1–N1A	97.24(17)
O4A–Co1–N1	87.28(18)	O4–Co1–N1	92.72(18)
O3B–Co1–N1	97.24(17)	O3C–Co1–N1	82.76(17)
N1A–Co1–N1	180.0		
2			
Ni1–N1	2.113(3)	Ni1–N1A	2.113(3)
Ni1–O3B	2.068(3)	Ni1–O3C	2.068(3)
Ni1–O4	2.062(3)	Ni1–O4A	2.062(3)
N1–Ni1–N1A	180.0	O3B–Ni1–O3C	180.0
O4–Ni1–O4A	180.0	O4–Ni1–N1A	93.12(12)
O3B–Ni1–O4	92.80(12)	O3C–Ni1–O4A	92.80(12)
O3C–Ni1–O(4)	87.20(12)	O3B–Ni1–O4A	87.20(12)
O3B–Ni1–N1	96.61(12)	O3C–Ni1–N1A	96.61(12)
O3C–Ni1–N1	83.39(12)	O3B–Ni1–N1A	83.39(12)
O4–Ni1–N1	86.88(12)	O4A–Ni1–N1A	86.88(12)
O4A–Ni1–N1	93.12(12)		

Symmetry codes: for **1**: A: $-x, -y+2, -z+2$; B: $x-1/2, -y+3/2, z+1/2$; C: $-x+1/2, y+1/2, -z+3/2$ and for **2**: A: $-x, -y, -z+2$; B: $-x+1/2, y-1/2, -z+3/2$; C: $x-1/2, -y+1/2, z+1/2$.

Table 3. Hydrogen bonds of **1** and **2**.

D–H...A	$d(\text{D}\cdots\text{H})$ (Å)	$\angle(\text{D–H}\cdots\text{A})$ (°)
1		
O5–H5...N3	2.831(7)	161(4)
O4–H4...O1	2.699(6)	170(7)
O4D–H4...O5	2.697(7)	170(7)
O5–H5...O3E	2.793(6)	150(4)
N2–H2...O2F	2.877(6)	148.6
2		
O5–H5...N3	2.787(5)	149(2)
O4–H4...O1	2.668(4)	165(4)
O4D–H4...O5	2.676(4)	164(4)
O5–H5...O3E	2.801(4)	157(3)
N2–H2...O2F	2.837(4)	151.0

Symmetry codes: D: $-x, 1-y, 2-z$; E: $x+1/2, 1/2-y, z+1/2$; F: $1-x, 1-y, 2-z$.

3. Results and discussion

3.1. Synthesis and general characterization

HL fusing purine and carboxyl groups for supermolecule assembly was synthesized via substitution of quantificational dideoxyinosine, chloroacetic acid, and sodium carbonate in water (scheme 1). The cleavage of the chiral (tetrahydrofuran-2-yl)methanol results in the unexpected **HL** which was fully determined by IR, ^1H NMR, and elemental analysis.

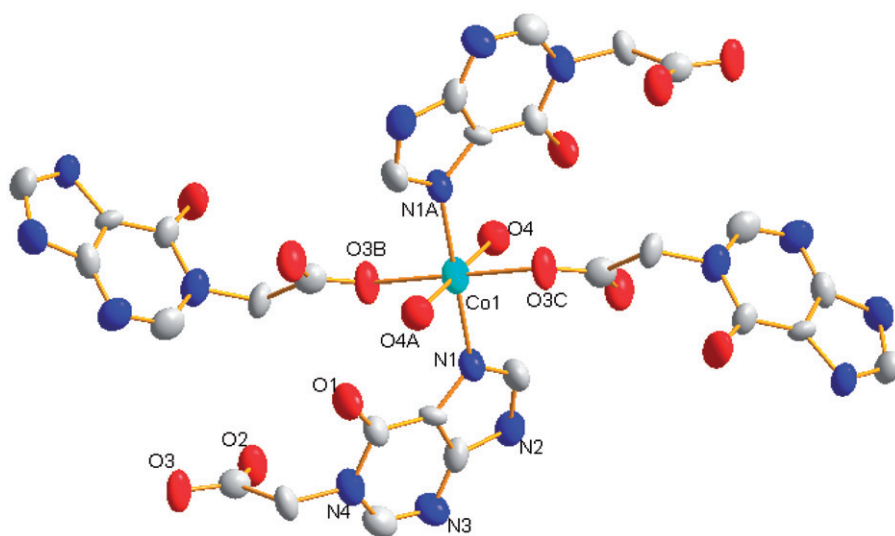


Figure 1. Coordination environment of the Co^{II} in **1** with hydrogen atoms and lattice water molecules omitted for clarity. Symmetry codes: A: $-x, -y + 2, -z + 2$; B: $x - 1/2, -y + 3/2, z + 1/2$; C: $-x + 1/2, y + 1/2, -z + 3/2$.

Preparation of **HL** underwent C–N bond cleavage as well as C–N bond formation. The C–N bond cleavage with formation of the nucleobase lacking the sugar moiety under the acid-catalyzed hydrolysis of 2'-deoxyguanosine was observed [15]. Removal of the (tetrahydrofuran-2-yl)methanol group from dideoxyinosine with C–N bond cleavage is inferred as a base-catalyzed hydrolysis reaction. Formation of a new C–N bond occurring at purine instead of imidazole indicates that strong electronic-abstraction of the carbonyl activates adjacent hydrogen attached at the imine, and makes it easily substituted by an acetic group.

Slow evaporation of the reaction mixtures of **HL**, ammonia, $\text{CoSO}_4 \cdot 7\text{H}_2\text{O}$, or $\text{NiSO}_4 \cdot 6\text{H}_2\text{O}$ in water/methanol for about three weeks led to two new coordination polymers **1** and **2**. For free **HL**, characteristic peak for vibration of C=O in acylamino is at 1685 cm^{-1} while characteristic vibrations of $-\text{COOH}$ and $\text{N}_{(\text{imidazole})}-\text{H}$ are at 1730 and 3129 cm^{-1} , respectively. IR spectra of **1** and **2** are similar. The middling absorptions at 3147 cm^{-1} for **1** and 3149 cm^{-1} for **2** are ascribed to $\text{N}_{(\text{imidazole})}-\text{H}$ while doubly strong absorptions at $1620\text{--}1670\text{ cm}^{-1}$ for **1** and **2** indicate vibration of C=O in the acylamino [16]. Strong absorptions at 1561 and 1381 cm^{-1} for **1** and at 1562 and 1383 cm^{-1} for **2** are due to $\nu_{\text{as}}(\text{COO}^-)$ and $\nu_{\text{s}}(\text{COO}^-)$ stretching vibrations, respectively, and the frequency differences between $\nu_{\text{as}}(\text{COO}^-)$ and $\nu_{\text{s}}(\text{COO}^-)$ suggest monodentate coordination of carboxylate [17]. IR data are in agreement with X-ray analyses.

3.2. Crystal structures of **1** and **2**

Single-crystal X-ray diffraction reveals **1** and **2** are isostructural, and thus only the structure of **1** is described in detail. Complex **1** crystallizes in the monoclinic $P2_1/c$ space group and is a 2-D coordination polymer. The asymmetric unit contains one-half Co^{II} , one deprotonated (**L**) $^-$, one coordinated water molecule, and one lattice water

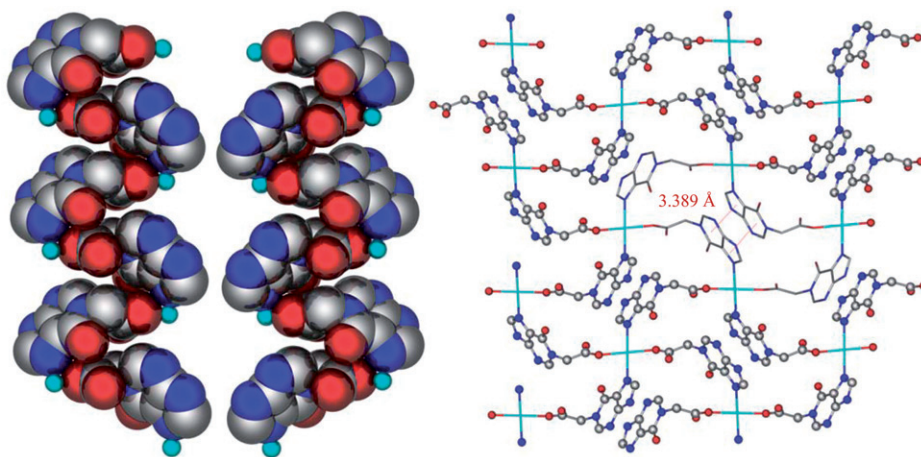


Figure 2. Left: space-filling view of right- and left-handed helical chains. Right: view of 2-D helical-constructed corrugated (4,4) sheets in **1** showing two helical conformations stabilized by strong π - π stacking interaction in one net expressly drawn as stick.

molecule. As shown in figure 1, every Co^{II} located at the inversion center i adopts a slightly distorted octahedral geometry coordinated by two nitrogen atoms and two oxygen atoms from four individual $(\text{L})^-$ [$\text{Co-N} = 2.203(5) \text{ \AA}$ and $\text{Co-O} = 2.103(5) \text{ \AA}$], and two oxygen atoms from two terminal water molecules [$\text{Co-O} = 2.094(4) \text{ \AA}$]. The bond lengths of Co-N and Co-O in **1** are normal values [18–20]. As for L^- , the acetate distorts from the purine plane with a dihedral angle of 81.8° and the flexible conformation of the ligand fabricates helical MOFs [18]. In **1**, each L^- serves as an angular bis-connector using one $\text{N}_{\text{imidazole}}$ and one $\text{O}_{\text{carboxyl}}$ to bridge the Co^{II} planar nodes with a separation distance of 9.143 \AA , and thereby forming a puckered metal-organic layer (figure 2). Further, as shown in figure 3, from the topological point of view, the layer of **1** is a uniform (4,4)-connected topology.

Each pair of adjacent Co^{II} is bridged by L^- to form two types of infinite helical chains running along the b -axis (see figures 2 and 3). The left- and right-handed helical chains are 2_1 helices with the helical pitch given by one full rotation of the 2-fold screw axis being 9.053 \AA , and hetero-helical chains are further linked through sharing common Co^{II} centers to form the puckered 2-D network (see figure 3). As represented in figure 2, each (4,4) net of the 2-D network in **1** is composed of two types of helical chains which not only wind through the common Co^{II} centers but also stabilize their helical conformations through stronger π - π stacking interaction between the two antiparallel purine groups in the net (the centroid-to-centroid distance being 3.389 \AA). Antiparallel stacking between adjacent purines forces the deprotonated carboxylates away from each other and reduces electric repulsion between anionic ligands $(\text{L})^-$.

Since metal-organic helical architectures have potential utilization in model materials, the construction for structures based on metal-organic helices have attracted growing interest [21]. Recently, various helical topologies involving the similar helical structures with the left- and right-handed strands sharing the common metal center have been found [22–25], but two helical conformations stabilized by stronger π - π stacking interaction in the same net of the MOFs and the purine-containing helical MOFs are rare [10a]. As shown in figure 4, those helical metal-organic layers are

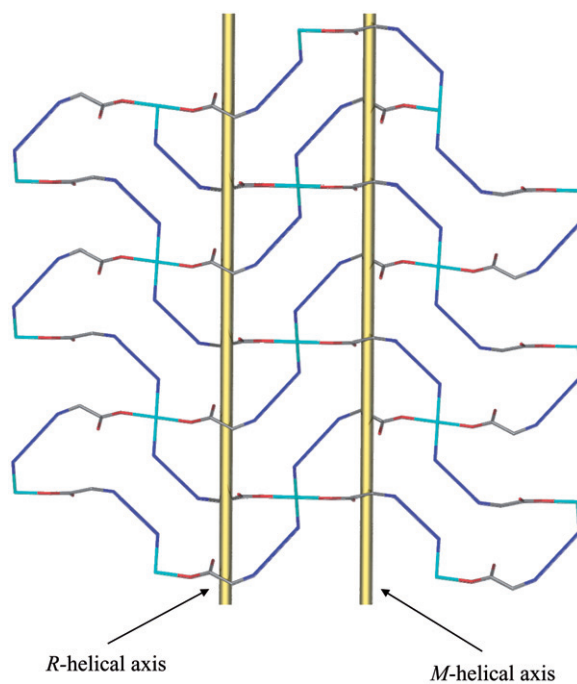


Figure 3. Schematic representation of the (4,4)-connected topology in **1** with the 2_1 helical axis of the metal-organic helix being drawn as the brass stick.

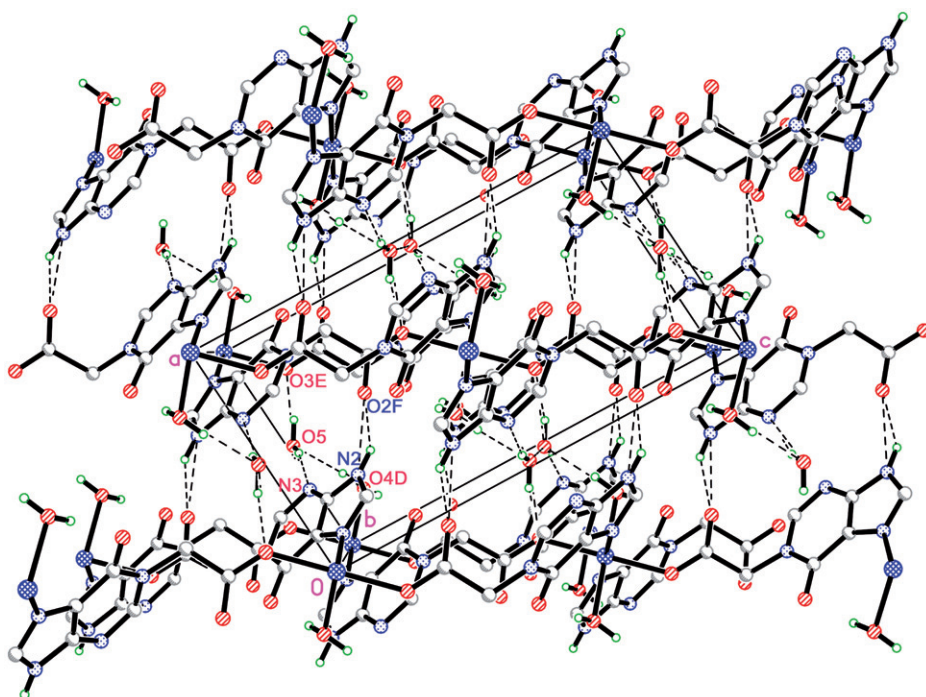


Figure 4. 3-D supramolecular network of **1** connected through interlayer hydrogen bonds of $N_{imidazole}^- \cdots H \cdots O_{carboxyl}$ and water-mediated interlayer hydrogen bonds.

extended into a 3-D supramolecular network through interlayer hydrogen bonds of $N_{\text{imidazole}}-\text{H}\cdots\text{O}_{\text{carboxyl}}$. Every lattice water molecule forms three hydrogen bonds with adjacent two layers, and thus this supramolecular network is further stabilized through water-mediated hydrogen-bonding interactions occurring between lattice water molecules and 2-D metal-organic layers.

3.3. XPRD and thermal stability analysis

The XPRD of **1** and **2** were measured, and the experimental and simulated XPRD patterns of the two complexes are presented in the “Supplementary material” section. The calculated XPRD patterns from single-crystal X-ray data are in agreement with the observed ones, indicating the phase purity of the synthesized powder products. The differences in intensity may be due to preferred orientation of the powder samples.

TGA data reveal that dehydration processes of **1** and **2** occurred at 157°C and 175°C, respectively (see “Supplementary material” section). For **1**, water molecules are completely removed up to 260°C, with the first weight loss of 13.1% corresponding to loss of the lattice and coordination water (*ca* 13.9%). With a plateau region at 260–392°C consecutive decomposition occurred at 392–517°C, suggesting total destruction of the framework. The remaining residue of 15.5% is supposed to be CoO (*ca* 14.5%) [26, 27]. However, **2** suffered from successive decomposition at 175–527°C. The remaining residue of 15.1% is considered to be NiO (*ca* 14.5%) [26, 28]. Although **1** and **2** are isostructural, slight differences in the strength of the interlayer hydrogen bonds and coordination bonds result in additional stability of **2** which can be detected by TGA (tables 2 and 3) [29].

3.4. Electronic spectra

The electronic absorption spectra of **HL** and complexes **1** and **2** were recorded in DMF (*ca* $1.0 \times 10^{-5} \text{ mol L}^{-1}$) at room temperature. As shown in the “Supplementary material” section, **1** and **2** show similar absorptions at 266 and 269 nm, respectively, in accord with the absorption of free **HL** at 266 nm. All observed absorptions of free ligand **HL** and complexes **1** and **2** are ascribed to $\pi \rightarrow \pi^*$ transitions associated with the aromatic rings of the ligand.

4. Conclusion

We have synthesized a purine-containing carboxylic acid **HL** and two new 2-D coordination polymers woven by two types of helically metal-organic chains sharing common metal centers. Through interesting π - π stacking and interlayer hydrogen-bond interactions originating from the bioactive purine group of **HL**, the 2-D coordination polymers are assembled into stable 3-D supramolecular networks of **1** and **2**, respectively. We are currently exploring supermolecular chemistry of **HL** with other metal ions.

Supplementary material

Crystallographic data for the structural analysis have been deposited with the Cambridge Crystallographic Data Centre, 855364 for **1** and 855365 for **2**. Copies of these information may be obtained free of charge from The Cambridge Crystallographic Data Centre *via* www.ccdc.cam.ac.uk/data_request/cif

Acknowledgments

We gratefully acknowledge financial support from the National Natural Science Foundation of China (20771094).

References

- [1] J.L. García-Giménez, M. González-Álvarez, M. Liu-González, B. Macías, J. Borrás, G. Alzuet. *J. Inorg. Biochem.*, **103**, 923 (2009).
- [2] J.T. Davis. *Angew. Chem. Int. Ed.*, **43**, 668 (2004).
- [3] P. Amo-Ochoa, O. Castillo, S.S. Alexandre, L. Welte, P.J. de Pablo, M.I. Rodríguez-Tapiador, J. Gomez-Herrero. *Inorg. Chem.*, **48**, 7931 (2009).
- [4] A. Bishop, O. Buzko, S. Heyeck-Dumas, I. Jung, B. Kraybill, Y. Liu, K. Shah, S. Ulrich, L. Witucki, F. Yang, C. Zhang, K.M. Shokat. *Annu. Rev. Biophys. Biomol. Struct.*, **29**, 577 (2000).
- [5] D. Choquesillo-Lazarte, M.P. Brandi-Blanco, I. García-Santos, J.M. González-Pérez, A. Castiñeiras, J. Niclós-Gutiérrez. *Coord. Chem. Rev.*, **252**, 1241 (2007).
- [6] R. Cejudo, G. Alzuet, M. González-Álvarez, J.L. García-Giménez, J. Borrás, M. Liu-González. *J. Inorg. Biochem.*, **100**, 70 (2006).
- [7] M. González-Álvarez, G. Alzuet, J. Borrás, L. del Castillo-Agudo, J.M. Montejó-Bernardo, A. Gutiérrez-Rodríguez, S. García-Granda. *J. Biol. Inorg. Chem.*, **13**, 1249 (2008).
- [8] B. Das, J.B. Baruah. *Cryst. Growth Des.*, **11**, 278 (2011).
- [9] E. Dubler, G. Hanggi, H. Schmalle. *Acta Crystallogr., Sect. C (Cr. Str. Comm.)*, **43**, 1872 (1987).
- [10] (a) E. Dubler, G. Hanggi, W. Bensch. *J. Inorg. Biochem.*, **29**, 269 (1987); (b) N. Okabe, M. Tsujita. *Acta Crystallogr., Sect. C (Cr. Str. Comm.)*, **56**, 1418 (2000).
- [11] (a) P. Mahata, M. Prabu, S. Natarajan. *Cryst. Growth Des.*, **9**, 3683 (2009); (b) H. Wu, H.Y. Liu, J. Yang, B. Liu, J.F. Ma, Y.Y. Liu, Y.Y. Liu. *Cryst. Growth Des.*, **11**, 2317 (2011); (c) S.S. Chen, J. Fan, T. Okamura, M.S. Chen, Z. Su, W.Y. Sun, N. Ueyama. *Cryst. Growth Des.*, **10**, 812 (2010).
- [12] (a) A.D. Naik, M.M. Dirtu, A. Léonard, B. Tinant, J. Marchand-Brynaert, B.L. Su, Y. Garcia. *Cryst. Growth Des.*, **10**, 1798 (2010); (b) Y. Akhriff, J. Server-Carrió, J. García-Lozano, J.V. Folgado, A. Sancho, E. Escrivà, P. Vitoria, L. Soto. *Cryst. Growth Des.*, **6**, 1124 (2006); (c) X.J. Wang, Z.M. Cen, Q.L. Ni, X.F. Jiang, H.C. Lian, L.C. Gui, H.H. Zuo, Z.Y. Wang. *Cryst. Growth Des.*, **10**, 2960 (2010); (d) Y.T. Wang, T.X. Qin, C. Zhao, G.M. Tang, T.D. Li, Y.Z. Cui, J.Y. Li. *J. Mol. Struct.*, **938**, 291 (2009).
- [13] (a) E. Dubler, G. Hanggi, W. Bensch. *J. Inorg. Biochem.*, **29**, 269 (1987); (b) N. Okabe, M. Tsujita. *Acta Crystallogr., Sect. C (Cr. Str. Comm.)*, **56**, 1418 (2000).
- [14] G.M. Sheldrick. *SHELX-97, Program for the Solution and Refinement of Crystal Structures*, University of Göttingen, Germany (1997).
- [15] (a) K.M. Schlitt, K.M. Sun, R.J. Paugh, A.L. Millen, L. Navarro-Whyte, S.D. Wetmore, R.A. Manderville. *J. Org. Chem.*, **74**, 5793 (2009); (b) J. Liu, C.J. Petzold, L.E. Ramirez-Arizmendi, J. Perez, H. Kenttämäa. *J. Am. Chem. Soc.*, **127**, 12758 (2005).
- [16] L. Wu, Y.H. Yu, X.J. Yuan, C.Q. Chu, B.L. Wu, H.Y. Zhang. *J. Coord. Chem.*, **64**, 2804 (2011).
- [17] B.S. Manhas, A.K. Tripathi. *J. Indian Chem. Soc.*, **LIX**, 315 (1982).
- [18] I.A. Guzei, A. Bakac. *Inorg. Chem.*, **40**, 2390 (2001).
- [19] G.V. Gibbs, R.T. Downs, D.F. Cox, K.M. Rosso, N.L. Ross, A. Kirfel, T. Lippmann, W. Morgenroth, T.D. Crawford. *J. Phys. Chem. A*, **112**, 8811 (2008).
- [20] S.A. Carabineiro, R.M. Bellabarba, P.T. Gomes, S.I. Pasco, L.F. Veiros, C. Freire, L.C.J. Pereira, R.T. Henriques, M.C. Oliveira, J.E. Warren. *Inorg. Chem.*, **47**, 8896 (2008).

- [21] (a) Y.Q. Lan, S.L. Li, Z.M. Su, K.Z. Shao, J.F. Ma, X.L. Wang, E.B. Wang. *Chem. Commun.*, **58** (2008); (b) B.L. Wu, L.Y. Meng, H.Y. Zhang, H.W. Hou. *J. Coord. Chem.*, **63**, 3155 (2010).
- [22] (a) Q.B. Bo, Z.X. Sun, G.L. Song, F. Li, G.X. Sun. *J. Inorg. Organomet. Polym.*, **17**, 615 (2007); (b) S.Q. Zang, Y. Su, Y.Z. Li, Z.P. Ni, Q.J. Meng. *Inorg. Chem.*, **45**, 174 (2006); (c) T.D. Owens, F.J. Hollander, A.G. Oliver, J.A. Ellman. *J. Am. Chem. Soc.*, **123**, 1539 (2001); (d) R.H. Wang, L.J. Xu, X.S. Li, Y.M. Li, Q. Shi, Z.Y. Zhou, M.C. Hong, A.S.C. Chan. *Eur. J. Inorg. Chem.*, 1595 (2004).
- [23] Y. Xu, L. Han, Z.Z. Lin, C.P. Liu, D.Q. Yuan, Y.F. Zhou, M.C. Hong. *Eur. J. Inorg. Chem.*, 4457 (2004).
- [24] X. Li, B.L. Wu, W. Liu, H.Y. Zhang. *Inorg. Chem. Commun.*, **11**, 1308 (2008).
- [25] J.H. Luo, Y.S. Zhao, H.W. Xu, T.L. Kinnibrugh, D. Yang, T.V. Timofeeva, L.L. Daemen, J.Z. Zhang, W. Bao, J.D. Thompson, R.P. Currier. *Inorg. Chem.*, **46**, 9021 (2007).
- [26] M.A. Nadeem, M. Bhadbhade, R. Bircher, J.A. Stride. *Cryst. Growth Des.*, **10**, 4063 (2010).
- [27] M.-H. Zeng, H.-H. Zou, S. Hu, Y.-L. Zhou, M. Du, H.-L. Sun. *Cryst. Growth Des.*, **9**, 4241 (2009).
- [28] D.P. Martin, M.A. Braverman, R.L. LaDuca. *Cryst. Growth Des.*, **7**, 2616 (2007).
- [29] M.V. Yigit, K. Biyikli. *Cryst. Growth Des.*, **6**, 63 (2006).